Jurnal Teknologi

Full Paper

PHOTOCATALYTIC REMOVAL OF PHENOL OVER MESOPOROUS ZnO/TiO_2 COMPOSITES

Klinsmann Cheong Lee Khang[a], Mohd Hayrie Mohd Hatta[a], Siew Ling Lee[a,b*], Leny Yuliati[c]

[a]Department of Chemistry, Faculty of Science, Universiti Teknologi Malaysia, 81310 UTM Johor Bahru, Johor, Malaysia
[b]Centre for Sustainable Nanomaterials, Ibnu Sina Institute for Scientific and Industrial Research, Universiti Teknologi Malaysia, 81310 UTM Johor Bahru, Johor, Malaysia
[c]Ma Chung Research Center for Photosynthetic Pigments, Universities Ma Chung, Malang 65151, Indonesia

Article history
Received
17 June 2017
Received in revised form
15 September 2017
Accepted
10 January 2018

Corresponding Author
sllee@ibnusina.utm.my

Graphical abstract

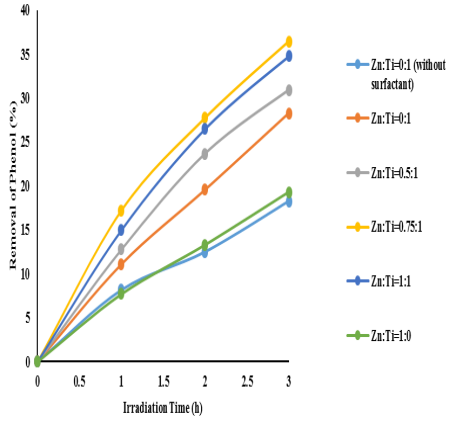

Abstract

A series of mesoporous ZnO/TiO_2 composites were successfully synthesized using cetyltrimethylammonium bromide surfactant. The composites of different Zn:Ti molar ratios (0.5:1, 0.75:1, and 1:1) were prepared by impregnating ZnO onto mesoporous TiO_2. XRD results verified co-existence of both anatase TiO_2 and hexagonal wurtzite ZnO in the ZnO/TiO_2 composites. Based on the Tauc plots, all the composites showed almost the same band gap energy of approximately 3.21 eV. The fourier transform infrared spectroscopy results successful covering of ZnO on the surface of the TiO_2 as the hydrophilicity property of TiO_2 decreased remarkably with the loading of ZnO in the composites. N_2 adsorption-desorption isotherms of the samples exhibited type-IV isotherm with a hysteresis loop. The Barrett-Joyner-Halenda pore size distribution revealed that the average pore size of the composites was around 3.6 nm, indicating the formation of mesopores dominantly in the samples. The photocatalytic removal of phenol over the samples under UV light irradiation after 3 h decreased in the order: ZnO/TiO_2 composites > anatase TiO_2 (with surfactant) > anatase TiO_2 (without surfactant) > ZnO. The composite with Zn:Ti molar ratio of 0.75:1 has achieved the highest photocatalytic activity of 36.5% in the removal of phenol under UV light irradiation for 3 h.

Keywords: TiO_2, ZnO, ZnO/TiO_2 composites, phenol, photocatalytic activity

Abstrak

Satu siri komposit berliang meso ZnO/TiO_2 telah berjaya disintesis menggunakan surfaktant bromida cetyltrimethylammonium (CTAB). Komposit daripada nisbah molar Zn/Ti yang berbeza (0.5:1, 0.75:1, dan 1:1) telah disediakan dengan pemuatan ZnO ke TiO_2 berkeliangan meso. Sebagai perbandingan, TiO_2 dengan/tanpa surfaktant dan ZnO juga telah disintesis. Corak XRD TiO_2 dengan/tanpa surfaktant mencadangkan pembentukan TiO_2 anatas, manakala corak XRD ZnO mengesahkan kehadiran wurtzit ZnO heksagon. Keputusan XRD juga mengesahkan kewujudan bersama kedua-dua TiO_2 anatasedan ZnO heksagon wurtzite dalam komposit ZnO/TiO_2. Berdasarkan plot Tauc, semua komposit menunjukkan tenaga jurang jalur yang hampir sama kira-kira 3.21 eV. Spektrum FTIR bagi komposit ZnO/TiO_2 menunjukkan bahawa ZnO berjaya meliputi pada permukaan TiO_2 dengan buktinya kepunyaan hidrofilik pada TiO_2 menurun ketara dengan pemuatan ZnO. Isoterma penjerapan-pendejerapan N_2 bagi komposit ZnO/TiO_2 mempamerkan

isoterma jenis keempat dengan gelung histerisis. Taburan saiz liang BJH yang diperolehi mencadangkan bahawa purata saiz liang bagi komposit lebih kurang 3.6 nm. Ini menunjukkan liang meso dominan dalam sampel. Penyingkiran fenol secara pemangkinan foto dengan sampel selepas 3 jam di bawah sinaran cahaya UV menurun dalam tertib: komposit ZnO/TiO_2 > TiO_2 anatase (dengan surfaktan)> TiO_2 anatas (tanpa surfaktan)> ZnO. Komposit dengan nisbah molar Zn:Ti sama dengan 0.75:1 telah mencapai aktiviti fotomangkin tertinggi sebanyak 36.5% dalam penyingkiran fenol di bawah cahaya penyinaran UV selama 3 jam.

Kata kunci: TiO_2, ZnO, komposit ZnO/TiO_2 , fenol, aktiviti fotomangkin

1.0 INTRODUCTION

Among various semiconductor oxides, TiO_2 has been recognized as one of the effective photocatalysts because it possesses high photocatalytic activity, low toxicity, high chemical stability and relatively low cost [1-3]. Fujishima (1972) reported that TiO_2, which was used as a photocatalytic anode, induced splitting of water efficiently into clean source of waste such as hydrogen and oxygen under ultraviolet light irradiation [4]. Thus, TiO_2 has attracted the interest of researchers to extensively investigate its photocatalytic activity for degradation of pollutants and production of hydrogen [5, 6]. The photocatalytic performance of TiO_2 can be greatly enhanced by modifications on its surface and coupling with other sulfides or oxides [7]. ZnO is one of the vital photocatalyst with a wide band gap (3.37 eV) as compared to TiO_2 (3.2 eV) [8]. ZnO has been proven to show the similar mechanism of photocatalytic degradation of organic pollutants [9].

ZnO/TiO_2 composites have been proven to achieve high efficient electron/hole pairs under irradiation and high photocatalytic activity [10]. In other words, the coupling of the two semiconductors is able to extend the duration period of the separation of electrons and holes with low recombination rate.

In this study, a series of mesoporous ZnO/TiO_2 composites were synthesized via wet impregnation method in order to remove phenol under ultraviolet light irradiation. The photocatalytic performance of the composites was evaluated through removal of phenol under ultraviolet light irradiation for 3 h.

2.0 METHODOLOGY

2.1 Preparation of Samples

TiO_2 (Zn:Ti=0:1) was synthesized via sol-gel method using CTAB surfactant. Firstly, 0.4375 g of CTAB was dissolved in 40 mL of ethanol. Then, 10 mL of titanium tetraisopropoxide (TTIP) and 0.5 mL of 1M HCl were added into the former mixture. After that, 4.5 mL of distilled water and 20 mL of ethanol were added into the precursor solution. The reaction mixture was left under stirring for an hour at room temperature. After an hour of continuous stirring, a gel was formed and aged at room temperature for 24 h. After a day of aging, the gel was then dried at 353 K for 8 hours. The sample was grinded and calcined at 773 K for 3 h in the rate of 1°C/min. This procedure was repeated without the addition of CTAB surfactant.

The TiO_2 synthesized with surfactant was then used to prepare ZnO/TiO_2 composites via wet impregnation method. The molar ratio of Zn/Ti was calculated based on the ratio of number of moles of zinc nitrate hexahydrate, $Zn(NO_3)_2.6H_2O$ to the number of moles of as-prepared TiO_2 that synthesized using surfactant. ZnO precursor was prepared by adding $Zn(NO_3)_2.6H_2O$ (x g) in distilled water (y mL) in a beaker. Sodium hydroxide, NaOH solution (1.0 M) was prepared by dissolving NaOH pellets (z g) in double distilled water (y mL) in a beaker. The amount of zinc nitrate hexahydrate, NaOH, and distilled water added corresponding to Zn:Ti= 0.5:1, 0.75:1, and 1:1 are recorded in Table 1. Before both the solutions were mixed and heated at 353 K with continuous stirring for 2 h, the as-prepared TiO_2 (1.0 g) was added into the mixture solution. The resulting mixture was aged at 370 K in oven for 24 h. The precipitated products were filtered using vacuum filtration and washed with double distilled water. The precipitates were then dried in oven at 370 K for 24 h. The precipitates were then calcined at 823 K. The calcination temperature was increased from room temperature to 823 K in the rate of 1°C/min, holding for 10 h. This procedure was used for the synthesis of ZnO without the addition of the TiO_2 that synthesized using surfactant.

Table 1 Amount of chemical used for the synthesis of ZnO/TiO_2 composites of different Zn/Ti molar ratios

Zn/Ti molar ratio	Mass of as-prepared TiO_2 (g)	x(g)	y(mL)	z(g)
0.5:1	1.0	1.900	12.78	0.5112
0.75:1	1.0	2.851	19.16	0.7663
1:1	1.0	3.802	25.56	1.0220

2.2 Characterizations of Photocataysts

The prepared samples were characterized using various types of instruments. A Bruker D8 Advance diffractometer with the Cu K_α (λ = 1.5405 Å) radiation as the diffracted monochromatic beam was used to record X-ray diffraction (XRD) patterns of the prepared samples in the 2θ range between 20° and 80° at a scan rate of 0.05° s^{-1}. A Shimadzu UV-2600 diffuse reflectance UV-Visible (DR UV-Vis) spectrophotometer was used to measure the absorption spectra of samples with barium sulphate ($BaSO_4$) as a reference. For determination of types of bonding, ATR FT-IR was used and performed using Thermo Scientific Nicolet iS10 FT-IR spectrometer. The spectra were recorded at the range from 400 to 4000 cm^{-1}. N_2 adsorption-desorption isotherms of the synthesized samples were characterized using NOVA Touch 4LX Surface Area and Pore Analyzer at -196 °C. The samples were degassed at 180 °C for 2 h under high vacuum before isotherm measurement. Brunauer-Emmett-Teller (BET) surface area of each sample was determined by a multipoint BET method using the adsorption data in the relative pressure (P/P°) range of 0-0.35. For determination of pore volume and average pore radius, desorption isotherm was used to determine the pore-size distribution via BJH method.

2.3 Photocatalytic Test

The photocatalytic activities of the prepared samples were evaluated for the removal of phenol under UV light irradiation. Phenol solution (53 mL) was then poured into an open glass reactor containing 50 mg of each of the samples. Prior to irradiation, the suspension was stirred in the dark for 30 min to establish an adsorption-desorption equilibrium condition between the organic molecules and the catalyst surface. After 30 min, 3 mL of the suspension was taken and filtered for the determination of its concentration which was interpreted from high-performance liquid chromatography (HPLC, Shimadzu Prominence LC-20A) equipped with a Hypersil GOLD PFP column monitored and diffuse reflectance UV-Visible (DR UV-Vis, Shimadzu UV-2600) spectrophotometer. The value was taken as initial concentration, A_0. When using DR UV-Vis, the full spectrum (250 – 800 nm) of each sample was recorded and the absorbance at selected wavelength (270 nm) was registered to determine phenol concentration. The suspension (50 mL) in an open glass reactor was then irradiated by UV light from the top (200 W Hg-Xe lamp, the dominant wavelength of UV light at 365 nm with light intensity of 16 mW/cm^2) for 3 h at room temperature. Amount of 3 mL of the suspension was withdrawn and filtered for every 1 hour until total of 3 h. The concentration of phenol at time t, A_t was determined and interpreted from its peak area and absorbance using high-performance liquid chromatography (HPLC, Shimadzu Prominence LC-20A) equipped with a Hypersil GOLD PFP column and diffuse reflectance UV-Visible (DR UV-Vis, Shimadzu UV-2600) spectrophotometer, respectively. The percentage of phenol removal was calculated according to the equation (1).

$$\frac{A_0 - A_t}{A_0} \times 100\% \quad (1)$$

where A_0 is the initial concentration of phenol after adsorption in dark condition, while A_t is the phenol concentration after UV light irradiation for t hour (t=1, 2, and 3 h).

3.0 RESULTS AND DISCUSSION

3.1 X-Ray Diffraction (XRD)

Figure 1 illustrates the XRD patterns of the samples synthesized at different Zn/Ti molar ratios. The XRD pattern of the TiO_2 synthesized without using surfactant confirmed the existence of anatase phase (PDF 00-021-1272) with the presence of sharp diffraction peaks located at 2θ = 25.3°, 38.0°, 48.1°, 54.1°, 55.1°, and 62.8°, which are corresponded to the (101), (004), (200), (105), (211), and (204) planes, respectively. The XRD pattern of the ZnO verified the formation of hexagonal wurtzite structure with the presences of sharp diffraction peaks located at 2θ = 31.7°, 34.3°, 36.1°, 47.5°, 56.6°, 62.8°, 66.3°, 67.9°, and 69.1°, which are corresponded to the (100), (002), (101), (102), (110), (103), (200), (112), and (201) planes, respectively. The pattern is indexed as hexagonal wurtzite ZnO phase (PDF 00-036-1451).

The XRD pattern of the TiO_2 synthesized using surfactant shows a peak at 2θ = 25.3° corresponding to the (101) reflection of anatase TiO_2. No other phase of rutile or brookite TiO_2 was observed. For ZnO/TiO_2 composites, the presence of the diffraction peaks of both anatase TiO_2 and wurtzite ZnO was confirmed in their XRD patterns. This was because a peak at 2θ = 25.3° corresponding to the (101) reflection of anatase TiO_2 and three peaks at 2θ = 31.7°, 34.3°, and 36.1° corresponding to (100), (002), and (101) planes of ZnO respectively, were identified. This implied that the composites consist of both TiO_2 and ZnO. No other impurity phase is present in the composite as evidence from the XRD diffraction pattern. As shown in Figure 1, the intensity of ZnO diffraction increased with an increase in the Zn/Ti molar ratio. This might be linked to the improved crystallinity and/or increased concentration of ZnO in the composition of the composites.

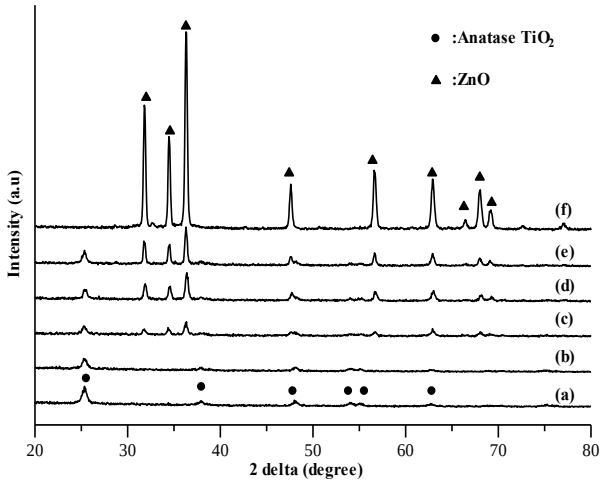

Figure 1 XRD patterns of ZnO/TiO2 composites (a) Zn:Ti=0:1 (without surfactant), (b) Zn:Ti=0:1, (c) Zn:Ti=0.5:1, (d) Zn:Ti=0.75:1, (e) Zn:Ti=1:1, and (f) Zn:Ti=1:0

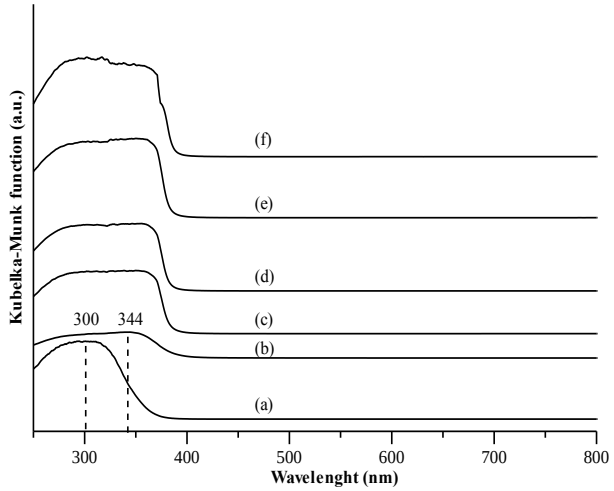

Figure 2 UV-Vis absorption spectra ZnO/TiO2 composites (a) Zn:Ti=0:1 (without surfactant), (b) Zn:Ti=0:1, (c) Zn:Ti=0.5:1, (d) Zn:Ti=0.75:1, (e) Zn:Ti=1:1, and (f) Zn:Ti=1:0

3.2 Diffuse Reflectance Ultraviolet Visible Spectrophotometer (DR UV-Vis)

The diffuse reflectance UV-Vis spectra of the samples expressed in terms of Kubelka-Munk function are shown in Figure 2. Based on the spectra, there was one major peak at around 300 nm for the TiO_2 synthesized without using surfactant. The spectra of TiO_2 synthesized with surfactant depicted an absorption peak at around 344 nm. The absorption peak of TiO_2 at around 300 nm was linked to the creation of octahedral or polymeric Ti species, which was also reported elsewhere [11]. For the TiO_2 synthesized using surfactant, the absorption peak red-shifted from 300 to 344 nm as compared to the TiO_2 synthesized without using surfactant. This was because nanoparticles with different morphology and particle size had different band gap energies [11]. ZnO exhibited wide absorption spectra range in the UV light region. The maximum absorption peak was observed at 317 nm and centered at 340 nm corresponding to the electronic transitions from valence band to the conduction band ($O_{2p} \rightarrow Zn_{3d}$) [12]. The ZnO/$TiO_2$ composites with Zn/Ti molar ratios of 0.5:1, 0.75:1, and 1:1 showed a combination of absorption peaks of TiO_2 that were synthesized using surfactant and ZnO.

Based on the UV-Vis absorption spectra, the effect of ZnO on the band gap energy (E_g) of the ZnO/TiO_2 composites was studied. The E_g was determined from Tauc plot by plotting $(ahv)^{2/n}$ versus hυ. The E_g of the samples were estimated based on the value of x-intercept by taking the linear extrapolation in the plot of $(ahv)^{1/2}$ versus hv, as shown in Figure 3. Table 2 lists the E_g values of the samples synthesized at different Zn:Ti molar ratios. The E_g of the TiO_2 synthesized using surfactant was higher than the TiO_2 synthesized without using surfactant. This was because after calcination at 773 K the surfactant was removed to give pore structure on the surface of the TiO_2, increasing its surface area. The nanoparticles with higher surface area have lower band gap energy as compared to the same nanoparticles with small surface area was reported [13]. The composites synthesized at Zn/Ti molar ratios of 0.5:1, 0.75:1, and 1:1, showed similar E_g of around 3.21 eV. The E_g of the composites were similar as the TiO_2 synthesized using surfactant and ZnO. This might be because the E_g of the TiO_2 and ZnO were similar to each other. Therefore, wet impregnation of the TiO_2 with ZnO has no significant effect on the band gap energy of the composites.

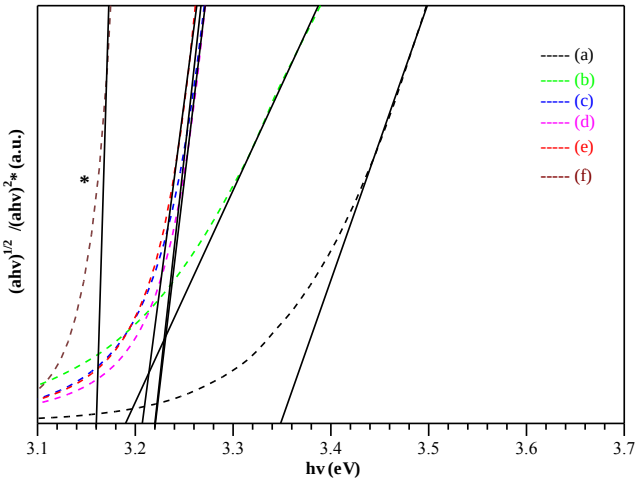

Figure 3 Tauc plots of ZnO/TiO2 composites (a) Zn:Ti=0:1 (without surfactant), (b) Zn:Ti=0:1, (c) Zn:Ti=0.5:1, (d) Zn:Ti=0.75:1, (e) Zn:Ti=1:1, and (f) Zn:Ti=1:0 (* refers to ZnO with direct band gap.)

Table 2 Band gap energy of ZnO/TiO_2 composites

Sample	Band gap energy (eV)
Zn:Ti=0:1 (without surfactant)	3.35
Zn:Ti=0:1	3.19
Zn:Ti=0.5:1	3.22
Zn:Ti=0.75:1	3.22
Zn:Ti=1:1	3.21
Zn:Ti=1:0	3.16

3.3 Fourier Transform Infrared Spectroscopy (FTIR)

Figure 4 shows the FTIR spectra of the samples synthesized at different molar ratios. The spectrum of the TiO_2 synthesized without using surfactant showed a band at 3423 cm^{-1} which was corresponded to stretching vibration of hydroxyl groups. Another peak observed in the spectrum at 1628 cm^{-1} was corresponded to the bending mode of hydroxyl groups. This is because the hydroxyl group and adsorbed water dominated the surface of the TiO_2. As observed in Figure 4, the intensity of these bands decreased with the increase of ZnO content in the sample. This implied that higher composition of ZnO reduced hydrophilicity property of the composites. In other words, the ZnO which was impregnated onto the TiO_2, was successfully covered the surface of the TiO_2 containing hydroxyl groups as evidence from the XRD analysis. The characteristic vibration of the inorganic Ti–O stretch was observed at 516 cm^{-1}. The spectrum of the ZnO depicted the characteristic peak of Zn-O at 423 cm^{-1}. For ZnO/TiO_2 composites, each of the spectrum illustrated a band at 440 - 472 cm^{-1} which was corresponded to metal oxide vibrations of TiO_2 and ZnO [1].

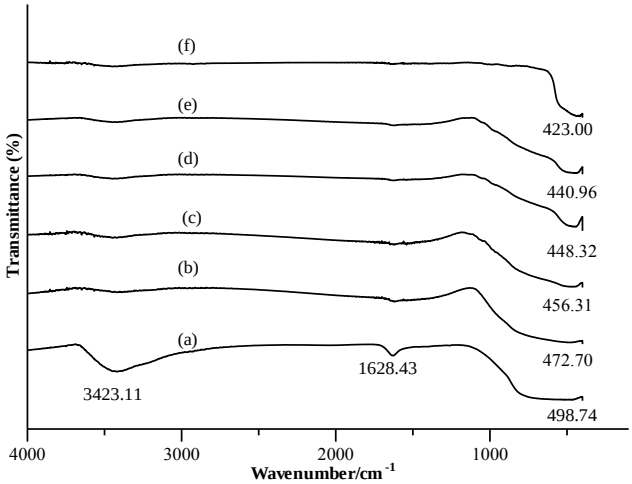

Figure 4 FTIR spectra of ZnO/TiO_2 composites (a) Zn:Ti=0:1 (without surfactant), (b) Zn:Ti=0:1, (c) Zn:Ti=0.5:1, (d) Zn:Ti=0.75:1, (e) Zn:Ti=1:1, and (f) Zn:Ti=1:0

3.4 Nitrogen Adsorption-Desorption Analysis

N_2 adsorption-desorption isotherms of the ZnO/TiO_2 composites synthesized at different Zn:Ti molar ratios are shown in Figure 5. From the isotherm, the type of porosity present in the synthesized samples could be determined. At high relative pressure (P/P^o>0.4), each of the composites exhibited a typical type-IV isotherm with a hysteresis loop. This indicates that the composites might consisted of mesoporous structure in abundance [14]. ZnO/TiO_2 composite with Zn:Ti molar ratio of 0:1 showed a H3 hysteresis loop in its isotherm, indicating the sample consists of slit shape pores with non-uniform size and/or shape. On the other hand, the isotherms of ZnO/TiO_2 composites synthesized at Zn:Ti molar ratios of 0.5:1, 0.75:1, and 1:1 showed a H4 hysteresis loop corresponding to uniform size and /or shape of slit shape pores.

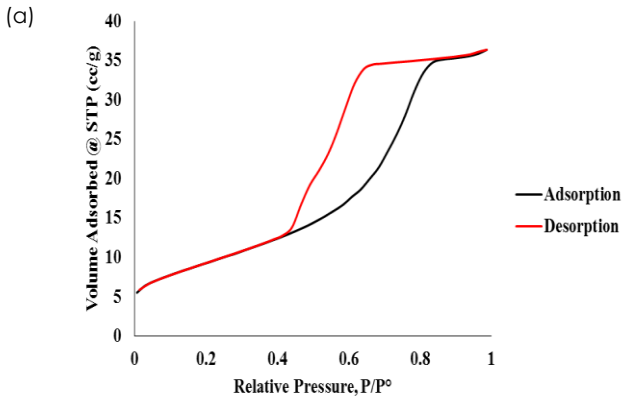

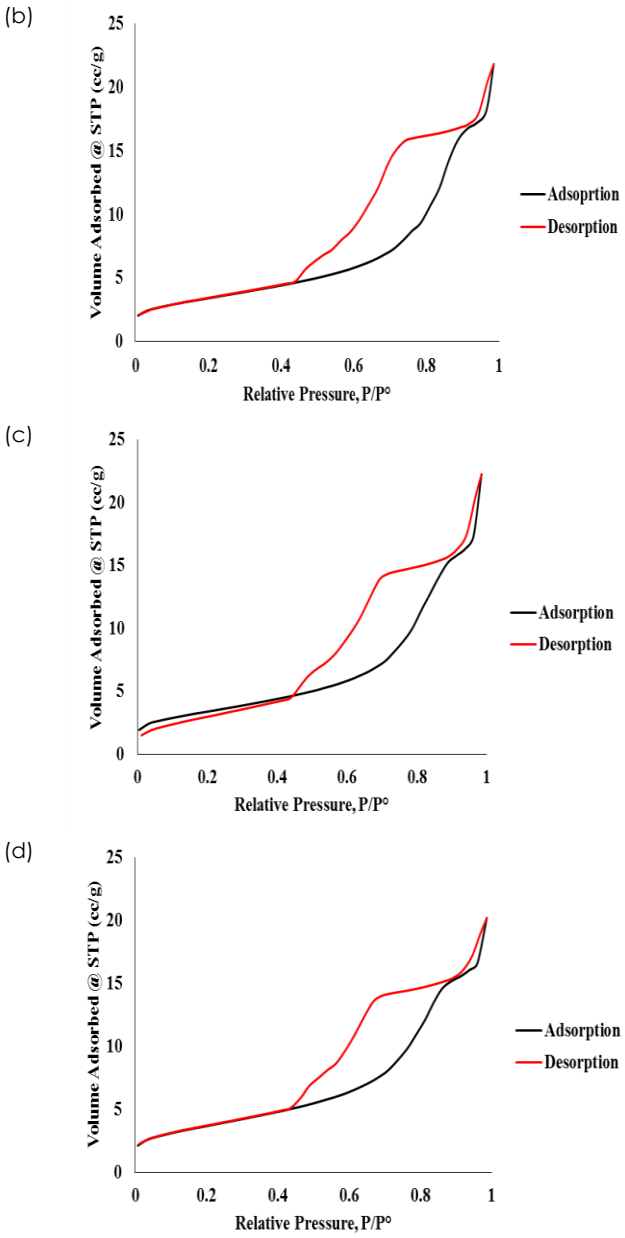

Figure 5 N_2 adsorption-desorption isotherms of ZnO/TiO2 composites synthesized with Zn/Ti molar ratios of (a) 0:1, (b) 0.5:1, (c) 0.75:1, (d) 1:1

The surface areas, pore volumes, and average pore sizes of the samples are recorded in Table 3. Figure 6 shows the BJH pore size distribution curves of the composites. The ZnO/TiO_2 synthesized at different Zn:Ti molar ratios have lower surface area and pore volume as compared to the TiO_2 with surfactant. The decrease in surface area and pore volume might be due to the deposition of ZnO inside the pores and formation of ZnO on the TiO_2 surface. This causes the blockage of pores to happen, leading to disruption of pore structure. The average pore radius of the prepared samples were almost the same except for the ZnO/TiO_2 synthesized at Zn:Ti molar ratio of 1:1. As compared to the TiO_2 with surfactant, the ZnO/TiO_2 synthesized at Zn:Ti molar ratio of 1:1 has larger average pore size of 3.840 nm. This might be due to the impregnation with ZnO selectively closed the smaller pores, leaving the larger pores for physisorption with N_2. This phenomenon is known as the confinement effect. The average pore sizes of the prepared samples were ranging 3.64 - 3.84 nm, indicating the existence of abundant mesopores in the composites.

Table 3 Surface area and pore data of ZnO/TiO2 composites

Sample	Surface Area (m^2/g)	Pore Volume (cm^3/g)	Average Pore Size (nm)
Zn:Ti=0:1	34	0.0648	3.64
Zn:Ti=0.5:1	12	0.0381	3.64
Zn:Ti=0.75:1	12	0.0391	3.63
Zn:Ti=1:1	13	0.0346	3.84

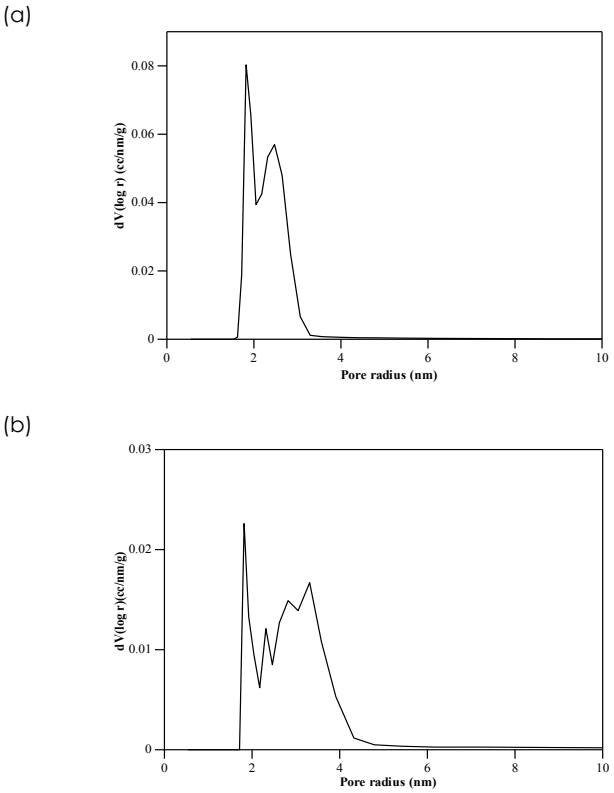

(c)

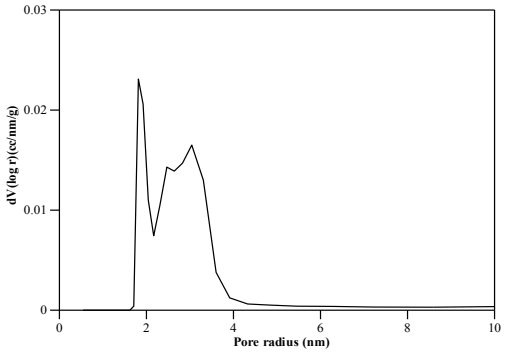

(d)

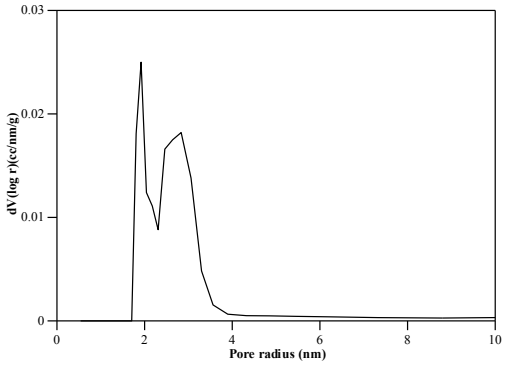

Figure 6 BJH pore size distribution curve of ZnO/TiO2 composites with Zn/Ti molar ratios of (a) 0:1, (b) 0.5:1, (c) 0.75:1, and (d) 1:1

3.5 Photocatalytic Testing

The ZnO/TiO_2 composites synthesized at different Zn/Ti molar ratios were evaluated for photocatalytic removal of phenol under UV light irradiation for 1-3 hours at room temperature. It was reported that phenol was not only stable under UV light irradiation, but also unable to be degraded under UV light irradiation without the photocatalyst [15]. On the other hand, adsorption test showed that adsorption-desorption equilibrium of phenol was achieved after 30 min of stirring under dark condition.

As depicted in Figure 7, after 3 h of UV light irradiation, it was shown that the percentage of removal of phenol over the TiO_2 synthesized without using surfactant and ZnO were 18.2% and 19.3%, respectively. Both samples showed similar photocatalytic performance under UV light irradiation. This might be attributed to the mechanisms of degradation of ZnO and TiO_2 which have been proven to be similar [7]. As compared to the TiO_2 synthesized without using surfactant, the TiO_2 synthesized using surfactant had higher percentage of removal of phenol, namely 28.3%. Synthesis of the TiO_2 synthesized using surfactant has improved the photocatalytic activity by 55.5% as compared to the TiO_2 synthesized without using surfactant. This was because the surface area of the TiO_2 synthesized using surfactant which functions as a size directing agent, was larger than that of TiO_2 synthesized without using surfactant, contributing to larger contact area of active sites for photocatalytic reaction to take place.

The ZnO/TiO_2 composites had higher photocatalytic activity in phenol removal than ZnO and the TiO_2 synthesized with/without surfactant. Among the composites, the composite synthesized at Zn:Ti molar ratio of 0.75:1 showed the highest percentage of removal phenol of 36.5% as compared to Zn:Ti=0.5:1 (30.9%) and Zn:Ti=1:1 (34.8%). Impregnation of the TiO_2 with ZnO has improved the photocatalytic activity by 29% as compared to the TiO_2 synthesized using surfactant. Apparently, the excellent photocatalytic activity of the composite related to the role of ZnO on the surface of the porous TiO_2.

In ZnO/TiO_2 composites, the electron transferred from the conduction band of light-activated ZnO to the conduction band of light-activated TiO_2. Conversely, hole transfer took place from the valence band of TiO_2 to the valence band of ZnO [16]. This efficient charge separation extended the duration period of the separation of electrons and holes, hence reducing the possibility of recombination of the charge species. Therefore, coupling of TiO_2 with ZnO increased the photocatalytic activity of ZnO/TiO_2 composite. Apart from that, the highest photocatalytic performance might also be contributed by the amount of ZnO, which is sufficient to trap the photogenerated electrons and prolong its lifetime. However, the composite with Zn:Ti=1:1 had a slightly lower percentage of removal of phenol as compared to Zn:Ti=0.75:1. It could be explained by possible coverage of TiO_2 sites ZnO which hindered the contact between TiO_2 and phenol, causing a decrease in the photocatalytic activity.

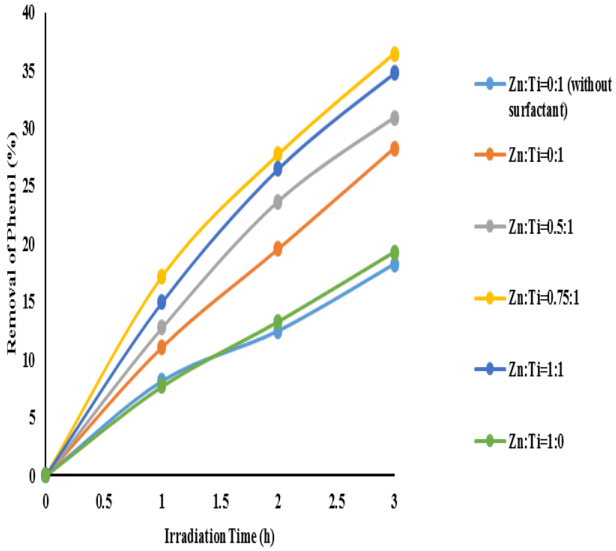

Figure 7 Photocatalytic removal of phenol over ZnO/TiO2 composites under UV light irradiation

4.0 CONCLUSION

A series of porous ZnO/TiO_2 composites synthesized at Zn/Ti molar ratio of 0.5:1, 0.75:1, and 1:1 was successfully prepared via wet impregnation of TiO_2 synthesized using surfactant with ZnO. The formation of anatase TiO_2 and wurtzite hexagonal ZnO were identified in the ZnO/TiO_2 composites. All the composites showed almost the same band gap energy of approximately of 3.21 eV. From N_2 adsorption-desorption analysis, the isotherm of ZnO/TiO_2 composites exhibited type-IV isotherm with a hysteresis loop. The BJH pore size distribution obtained revealed that the average pore radii of the composites were around 3.6 nm, indicating the presence of mesopores in the composites. The composite with Zn:Ti molar ratio of 0.75:1 was found to achieve the highest photocatalytic activity of 36.5% in the removal of phenol under UV light irradiation for 3 h. The high photocatalytic activity obtained on the composite with Zn:Ti molar ratio of 0.75:1 could be due to efficient charge separation and suppressed electron-hole recombination on the TiO_2.

Acknowledgement

This work has been financially supported by Ministry of Higher Education (MOHE) and Universiti Teknologi Malaysia through Research University Grants (vote no. Q.J130000.2526.12H77 and Q.J130000.2526.13H52).

References

[1] Li, X., Lv, K., Deng, K., Tang, J., Su, R., Sun, J., & Chen, L. (2009). Synthesis and Characterization of ZnO and TiO_2 Hollow Spheres with Enhanced Photoreactivity. *Materials Science and Engineering: B*. 158(1). 40-47.

[2] Koh, P. W., Yuliati, L., Lintang, H. O., Lee, S. L. 2015. Increasing Rutile Phase Amount in Chromium-doped Titania by Simple Stirring Approach for Photodegradation of Methylene Blue under Visible Light. *Australian Journal of Chemistry*. 68. 1129-1135.

[3] Ooi, Y. K., Yuliati, L., Lee, S. L. 2016. Phenol Photocatalytic Degradation over Mesoporous TUD-1-supported Chromium Oxide-doped Titania Photocatalyst. *Chinese Journal of Chemistry*. 37: 1871-1881.

[4] Fujishima, A. 1972. Electrochemical Photolysis of Water at a Semiconductor Electrode. *Nature*. 238: 37-38.

[5] Yu, T., Tan, X., Zhao, L., Yin, Y., Chen, P., & Wei, J. 2010. Characterization, Activity and Kinetics of a Visible Light Driven Photocatalyst: Cerium and Nitrogen Co-doped TiO_2 Nanoparticles. *Chemical Engineering Journal*. 157(1): 86-92.

[6] Lin, S., Shi, L., Yoshida, H., Li, M., & Zou, X. 2013. Synthesis of Hollow Spherical Tantalum Oxide Nanoparticles and Their Photocatalytic Activity for Hydrogen Production. *Journal of Solid State Chemistry*. 199: 15-20.

[7] Kanjwal, M. A., Barakat, N. A., Sheikh, F. A., Park, S. J., & Kim, H. Y. 2010. Photocatalytic Activity of ZnO-TiO_2 Hierarchical Nanostructure Prepared by Combined Electrospinning and Hydrothermal Techniques. *Macromolecular Research*. 18(3): 233-240.

[8] Zhang, M., An, T., Hu, X., Wang, C., Sheng, G., & Fu, J. 2004. Preparation and Photocatalytic Properties of a Nanometer ZnO–SnO_2 Coupled Oxide. *Applied Catalysis A: General*. 260(2): 215-222.

[9] Logothetidis, S., Laskarakis, A., Kassavetis, S., Lousinian, S., Gravalidis, C., & Kiriakidis, G. 2008. Optical and Structural Properties of Zno for Transparent Electronics. *Thin Solid Films*. 516(7): 1345-1349.

[10] Zhang, M., An, T., Liu, X., Hu, X., Sheng, G., & Fu, J. 2010. Preparation of a High-activity ZnO/TiO_2 Photocatalyst via Homogeneous Hydrolysis Method with Low Temperature Crystallization. *Materials Letters*. 64(17): 1883-1886.

[11] Valencia, S., Marín, J. M., & Restrepo, G. 2010. Study of the Bandgap of Synthesized Titanium Dioxide Nanoparticles Using the Sol-gel Method and a Hydrothermal Treatment. *Open Materials Science Journal*. 4(1): 9-14.

[12] Dutta, S., & Ganguly, B. N. 2012. Characterization of ZnO Nanoparticles Grown in Presence of Folic Acid Template. *Journal of Nanobiotechnology*. 10(1): 29.

[13] Prabhu, Y. T., Rao, K. V., Kumar, V. S. S., & Kumari, B. S. 2013. Synthesis of ZnO Nanoparticles by a Novel Surfactant Assisted Amine Combustion Method. *Advances in Nanoparticles*. 2(01): 45.

[14] Samantaray, S. K., Mohapatra, P., & Parida, K. 2003. Physico-chemical Characterisation and Photocatalytic Activity of Nanosized SO_4^{2-}/TiO_2 Towards Degradation of 4-nitrophenol. *Journal of Molecular Catalysis A: Chemica*. 198(1): 277-287.

[15] Alim, N. S., Lintang, H. O., & Yuliati, L. 2016. Photocatalytic Removal of Phenol Over Titanium Dioxide-reduced Graphene Oxide Photocatalyst. *IOP Conference Series: Materials Science and Engineering*. 107(1): 012001. IOP Publishing.

[16] Serpone, N., Maruthamuthu, P., Pichat, P., Pelizzetti, E., & Hidaka, H. 1995. Exploiting the Interparticle Electron Transfer Process in the Photocatalysed Oxidation of Phenol, 2-Chlorophenol and Pentachlorophenol: Chemical Evidence for Electron and Hole Transfer Between Coupled Semiconductors. *Journal of Photochemistry and Photobiology A: Chemistry*. 85(3): 247-255.